PHYSICAL REVIEW A **92**, 031601(R) (2015)

Quantum impurity in a one-dimensional trapped Bose gas

A. S. Dehkharghani,[1] A. G. Volosniev,[1,2] and N. T. Zinner[1,*]
[1]*Department of Physics and Astronomy, Aarhus University, DK-8000 Aarhus C, Denmark*
[2]*Institut für Kernphysik, Technische Universität Darmstadt, D-64289 Darmstadt, Germany*
(Received 23 March 2015; published 29 September 2015)

We present a theoretical framework for describing an impurity in a trapped Bose system in one spatial dimension. The theory handles any external confinement, arbitrary mass ratios, and a weak interaction may be included between the Bose particles. To demonstrate our technique, we calculate the ground-state energy and properties of a sample system with eight bosons and find an excellent agreement with numerically exact results. Our theory can thus provide definite predictions for experiments in cold atomic gases.

DOI: 10.1103/PhysRevA.92.031601 PACS number(s): 03.75.Mn, 68.65.−k, 67.85.Pq

An impurity interacting with a reservoir of quantum particles is an essential problem of fundamental physics. Famous examples include a single charge in a polarizable environment, the Landau-Pekar polaron [1,2], a neutral particle in superfluid ^{4}He [3], a magnetic impurity in a metal resulting in the Kondo effect [4], and a single scattering potential inside an ideal Fermi gas [5,6]. The latter system is famous for the Anderson's orthogonality catastrophe [7]. In these settings the impurity behavior can provide key insights into the many-body physics and guide our understanding of more general setups.

A complicating feature of many impurity problems is the presence of interactions at a level that often precludes the use of perturbative analysis and self-consistent mean-field approximations. This implies that analytical approaches are highly desirable and exact solutions are, when available, coveted tools for benchmarking other techniques. This is particularly true for one-dimensional (1D) homogeneous systems where solutions can often be found based on the Bethe ansatz [8–13]. These solutions are the essential ingredients for our analytical understanding of highly controllable experiments with cold atoms [14–19]. For instance, the exactly solvable problem of the single impurity in a 1D Fermi sea [10]—the Fermi polaron—can be used to study the atom-by-atom formation of a 1D Fermi sea [20].

While Fermi polarons have been studied intensively in recent times using cold atomic setups both experimentally and theoretically [21–25], the physics of impurities in a bosonic environment is only now becoming a frontier in cold atom experiments [26–29]. This pursuit requires theoretical models for describing the Bose polaron [30–48], where, in contrast to the Fermi polaron, an exact solution is not known even for a homogeneous 1D system. Here, we provide a theoretical framework that captures the properties of an impurity in a bosonic bath confined in one spatial dimension. Our (semi)analytical theory thus provides a state-of-the-art tool for exploring the properties of Bose polarons in 1D.

The proposed framework works with a zero-range potential of any strength and handles any number of majority particles in external confinement of various shapes. Our method is also applicable to describe experimental setups that have different trapping potentials for the impurity and majority particles and different mass ratios. In addition, weak majority interactions may be included using the well-known Gross-Pitaevskii equation (GPE). While our method is not exact, we have benchmarked the energetics and density profiles against numerical results [40] and find agreement for up to ten particles at the level of a few percent. To illustrate the method in this Rapid Communication, we examine a system of eight bosons and an impurity in a harmonic trap. Figure 1(a) shows a sketch of this system with vanishing boson-boson and large boson-impurity interactions. This leads to a separation of the two components. Notice that the ground state must retain parity and is thus a linear superposition of the two spatial configurations outlined. Using the pair-correlation function, we can clearly see in Figs. 1(b)–1(d) how the impurity moves to the edge of the system as a function of the interspecies interaction. Increasing the intraspecies interaction, we witness the opposite effect as the impurity goes to the center of the system, as seen in Figs. 1(e)–1(g).

Formalism. Our two-component system consists of one type A (impurity), and N_B identical type B bosons (majority) with masses m_A and m_B, respectively. For the sake of argument, we confine particles in harmonic potentials with a trapping frequency ω_B for the bosons and ω_A for the impurity. In this Rapid Communication we adopt harmonic oscillator units for the majority particles, i.e., we measure length in units of $b = \sqrt{\hbar/m_B\omega_B}$ and energy in units of $\hbar\omega_B$. Accordingly, the Hamiltonians, for the impurity atom with coordinate x and a majority atom with coordinate y, are expressed as

$$H_A(x) = \frac{p_x^2 + m_{AB}^2\omega_{AB}^2 x^2}{2m_{AB}}, \quad H_B(y) = \frac{p_y^2 + y^2}{2}, \tag{1}$$

where $m_{AB} = m_A/m_B$, $\omega_{AB} = \omega_A/\omega_B$, and p denotes the corresponding momenta. The interaction between A and B particles is assumed to be of a short range and hence modeled by the Dirac delta function with strength g. The boson-boson interaction is also given in the standard pseudopotential interaction model [49] with a coupling constant g_{BB}. Both interaction strengths are given in units of $[b\hbar\omega_B]$. The overall Hamiltonian of the system is $H = H_A(x) + \sum_{i=1}^{N_B} H_B(y_i) + \sum_{i=1}^{N_B} g\delta(x - y_i) + \sum_{i<k} g_{BB}\delta(y_i - y_k)$, where y_i are the coordinates of the bosons (see the Supplemental Material [50]).

In order to find the eigenspectrum of the Hamiltonian for arbitrary g, we introduce a (semi)analytical approach. More specifically, we consider the impurity as the "slow" variable and introduce the adiabatic decomposition of the total wave

*zinner@phys.au.dk

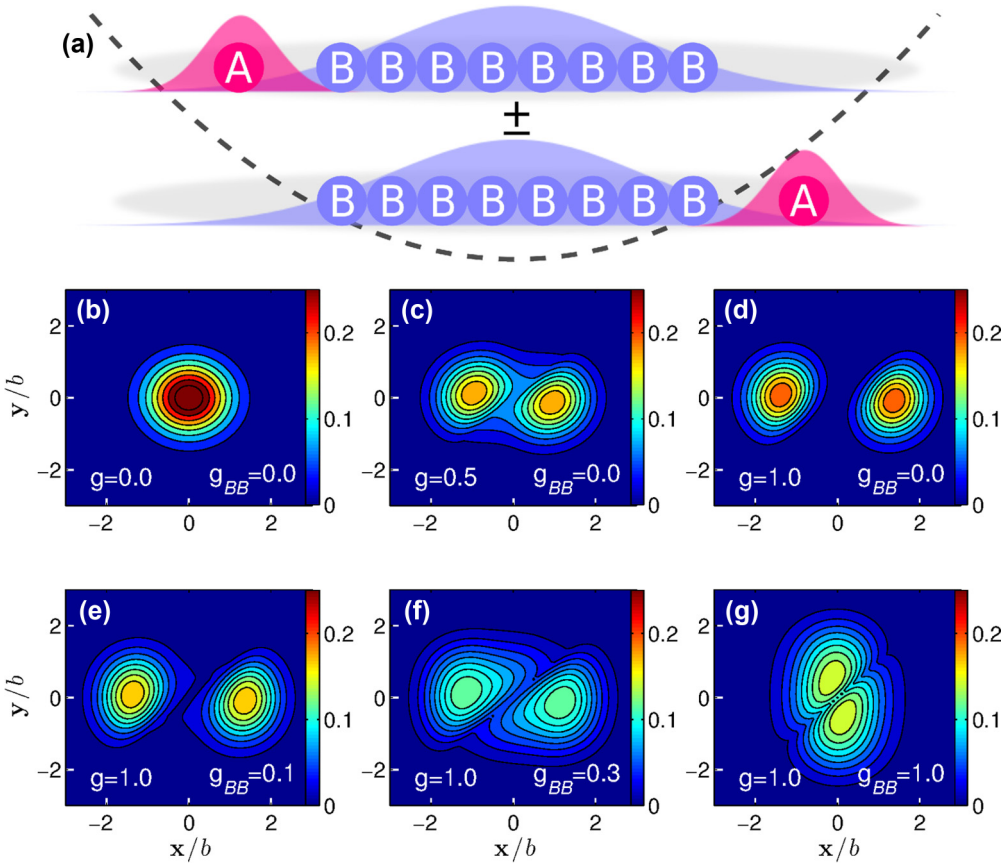

FIG. 1. (Color online) (a) A sketch of the doubly degenerate ground state for the system of one A and eight B particles trapped in a one-dimensional harmonic potential for infinitely strong repulsive interspecies interactions. The $\pm$ corresponds to the parity of the system. (b)–(d) show the AB pair-correlation function, the expectation value of the $\delta(z_A - x)\delta(z_B - y)$ operator, where $z_{A(B)}$ is the coordinate of particle $A(B)$. The system under consideration is the same as in (a) although with a finite interspecies interaction strength g. (e)–(g) show the pair-correlation function for different intraspecies interaction strengths g_{BB} for fixed g.

function

$$\Psi(x, y_1, \ldots, y_{N_B}) = \sum_{j=1} \phi_j(x)\Phi_j(y_1, \ldots, y_{N_B}|x), \quad (2)$$

where Φ_j is the jth normalized eigenstate of the eigenvalue problem $\sum_{i=1}^{N_B} H_B(y_i)\Phi_j = E_j(x)\Phi_j$, which we solve assuming that the impurity gives rise to a zero-range potential at a fixed position x (see the Supplemental Material [50]). First, we consider an ideal Bose gas, i.e., $g_{BB} = 0$, and write $\Phi_j(y_1, \ldots, y_{N_B}|x) = \hat{S}\prod_{i=1}^{N_B} f_{k_i^j}(y_i|x)$ with a symmetrization operator $\hat{S}$ (acting on the y_i coordinates) and $f_{k_i^j}(y_i|x)$ being the k_i^jth normalized eigenstate of $H_B(y_i)$ for a given x. Notice that every function $f_{k_i^j}(y_i|x)$ has a discontinuous derivative at $y_i = x$ due to the zero-range interaction. This is quantified with the standard delta-function boundary condition, which dictates that the difference in the slopes of the wave function, from the left and right sides of x, times a $1/(2g)$ factor must be equal to the value of the wave function taken at $y_i = x$. As $1/g \to 0$, the wave function must therefore vanish at $y_i = x$.

We can include interactions among the majority particles under the assumption that these may be described by the 1D GPE (see the Supplemental Material [50]). It has been previously discussed that this is an accurate description for weak interactions between the bosons [51–53]. In this case we need to use a dressed single-particle wave function $\tilde{f}_{k_i^j}$ instead of $f_{k_i^j}(y_i|x)$. The function $\tilde{f}_{k_i^j}$ satisfies the 1D GPE complemented with the boundary condition at $y_i = x$,

$$\mu(x)\tilde{f}_{k_i^j} = \left(-\frac{1}{2}\frac{\partial^2}{\partial y_i^2} + \frac{1}{2}y_i^2 + N_B g_{BB}\left|\tilde{f}_{k_i^j}\right|^2\right)\tilde{f}_{k_i^j}, \quad (3)$$

where $\mu(x)$ is a chemical potential, and g_{BB} is determined through the three-dimensional boson-boson scattering length a_s as $g_{BB} = \frac{2a_s}{b}\frac{\sqrt{\omega_{B_1}\omega_{B_2}}}{\omega_B}$, where ω_{B_1} and ω_{B_2} are the two frequencies in the directions of strong confinement [54]. The boson-impurity coupling constant can be also related to the corresponding scattering length [55].

After determining the function $f_{k_i^j}$, we obtain a coupled system of equations for $\phi_j(x)$ (see the Supplemental Material [50]). The coupling terms in this system correspond to the transition of a majority particle from f_k to $f_{k'}$. For bosons, this is a coherent process which contributes significantly if the impurity is placed in a region with a high density of majority particles. Physical intuition, however, tells us that, in the ground and low-lying excited states, the impurity is pushed to the edge of the trap if $g_{BB} \ll g$ and $N_B \gg 1$.

Otherwise, the impurity would deplete the majority particles notably from the ground state of the one-body harmonic oscillator, which is very expensive energywise for $N_B \gg 1$. Hence, for large N_B, we neglect the coupling terms between different $\phi_j(x)$, which rigorously gives us an upper bound for the exact energy of the ground state [56]. However, we expect this approximation to be very accurate also for low-lying excited states. We can therefore obtain $\phi_j(x)$ by solving numerically a single differential equation. From a mathematical point of view, the presented approach is similar to the Born-Oppenheimer approximation or the hyperspherical adiabatic method [57]. The physics is, however, different. Indeed, we develop our method for a many-body system where we expect that for the same computational time the relative precision is increasing with the number of particles. Clearly, the discussion above applies to a Bose polaron problem in arbitrary confinement. Moreover, the trapping potentials as well as the masses can be different for the A and the B particles. Below, we show that our framework compares very well to exact numerical results for the equal mass case $m_A = m_B$. In the heavy impurity case with $m_A > m_B$, we expect our model to perform equally well as the impurity becomes increasingly stationary. The final case of a light impurity $m_A < m_B$ will not be studied further here, but we note that since it must also go to the edge of the trap, the arguments above for neglecting coupling terms still hold. We have checked that we get the expected separation (the light impurity goes to the edge of the trap), although further studies will have to be conducted to investigate the quantitative performance of our method for light impurities.

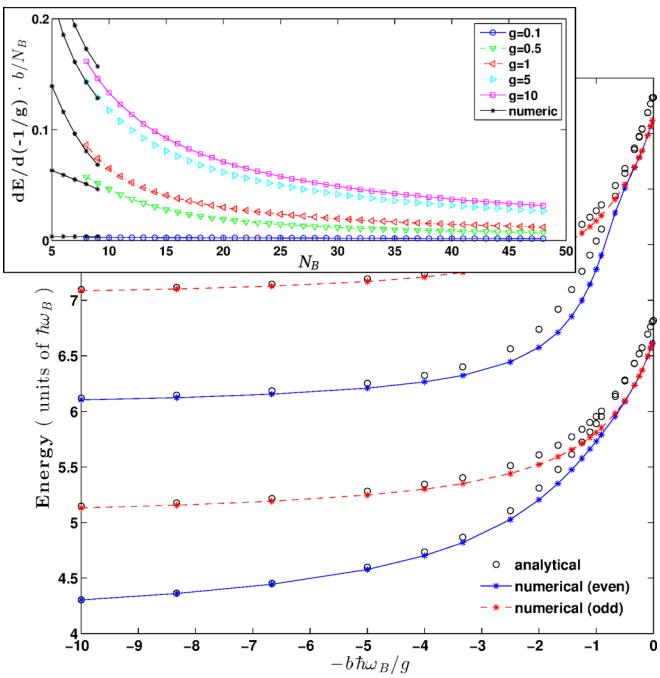

FIG. 2. (Color online) The energy spectrum of low-lying states for a system of eight noninteracting bosons and an impurity with $m_{AB} = \omega_{AB} = 1$. The inset shows the derivative of the ground-state energy $\partial E/\partial(-1/g)$ divided by N_B, which is related to Tan's contact parameter. The lines are guides for the eye.

To conclude the presentation of our method, we compare its predictions with the exact results obtained using the numerical approach developed in Refs. [40,58] for $g_{BB} = 0$, $m_{AB} = \omega_{AB} = 1$. We find that the relative precision of the method increases with N_B and we pick a sample system with $N_B = 8$. We start by analyzing the energies in Fig. 2. Our model yields results that are slightly above the numerically exact values with a maximum deviation of a few percent. Next, we check that the model reproduces the derivative of the ground-state energy with respect to the coupling constant $\partial E/\partial(-1/g)/N_B$ vs N_B (see the inset in Fig. 2). This derivative for fixed g determines the probability for a given boson to be close to the impurity [59,60]. We see that for a large number of bosons this probability becomes smaller, manifesting that the impurity is pushed far from the center of the trap. It is also interesting to note that for large N_B we find numerically that $\partial E/\partial(-1/g)$ is almost independent of N_B.

We have also compared density profiles and pair-correlation functions for the ground state and again find only minute differences [see Figs. 3(a) and 3(b)]. Note that the impurity density splits for large g. On the other hand, the majority particles are almost unperturbed by the interaction. This means that an adiabatically slow increase of g moves the impurity to the edge of the system, as also shown in Figs. 1(a)–1(d). As the number of bosons increases, the impurity gets pushed further towards the edge of the trap, and $\partial E/\partial(-1/g)/N_B$ decreases. In the energy domain it leads to a doubly degenerate ground

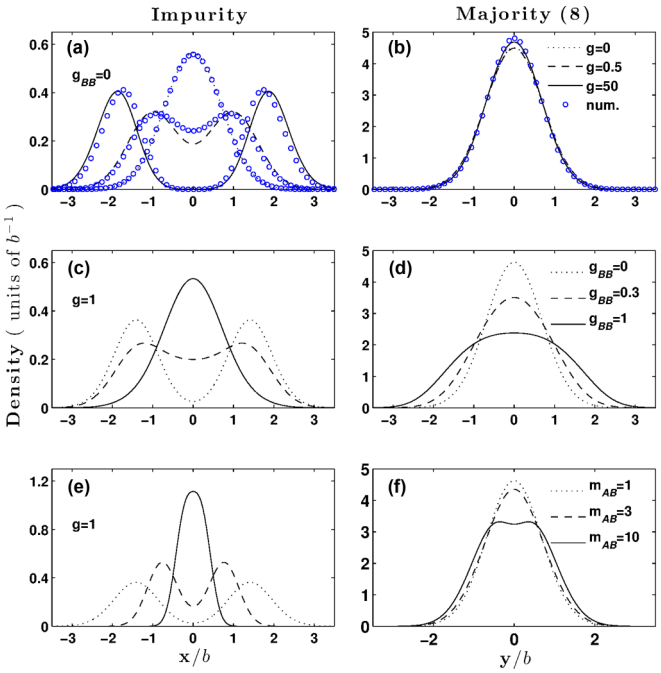

FIG. 3. (Color online) (a) and (b) show the density distributions for the (a) impurity and (b) majority atoms for $N_B = 8$ and different values of the interspecies interaction strength g. The numerically exact results are shown with blue dots in (a) for the three corresponding values of g, and in (b) for $g = 50$. Notice that the label in (a) also applies to (b) and vice versa. (c), (d) The density distributions for a fixed value of $g = 1$ but different intraspecies interaction strengths g_{BB}. (e)–(f) The density distributions for different values of mass ratios, $m_{AB} = 1$, 3, and 10, with $g_{BB} = 0$.

state at $1/g = 0$ since the impurity can be pushed to either the left or the right edges of the trap; see Figs. 1(a) and 2. This should be contrasted with the Fermi polaron system, where for large interactions the ground state is $N_B + 1$ times degenerate and the impurity is localized in the middle of the trap [58,61,62].

Results. To further illustrate the model, we continue our discussion of an impurity interacting with eight bosons. However, now we allow a weak interaction between the bosons as well as different mass (or frequency) ratios. For large interactions this setup is already beyond current numerical approaches. We stress once again that in our method the numerical complexity does not increase with N_B, and $N_B = 8$ is chosen as a particular example.

First, we fix $g = 1$, $m_{AB} = 1$, $\omega_{AB} = 1$, and change the intraspecies interaction strength g_{BB}. In Figs. 3(c) and 3(d) we show the density for the impurity and majority atoms in the ground state. In this case the energy is minimized if the impurity is pushed towards the middle of the trap. This is readily understood for the case $g = g_{BB}$, where the impurity particle should have the same density distribution due to the boson-impurity exchange symmetry of the Hamiltonian. In our case the difference in the densities of majority and impurity for $g = g_{BB} = 1$ is due to the different treatments of these components. Notice also that we expect the GPE and our approach to yield only qualitative results for such a large boson-boson interaction strength. It is also worth noticing that if both interactions g and g_{BB} are very large, one can approach the problem directly by using the Bose-Fermi mapping [63], where one also expects enhancement of the impurity density in the middle of the trap compared to the $g_{BB} = 0$ case. Next, we compute the pair-correlation function which again demonstrates that the impurity is situated close to the origin; see Figs. 1(e)–1(g). Consider now different masses for A and B particles for $g_{BB} = 0$, $g = 1$, and $\omega_{AB} = 1$ [64]. As shown in Figs. 3(e)–3(f), when m_{AB} becomes larger, the external potential localizes the impurity in the middle of the system. For $m_{AB} \to \infty$ the impurity constitutes a delta-function barrier in the middle of the harmonic trap, the solution to which can be found in Ref. [65]. From this picture it is apparent that the density of the majority particles should be suppressed at the origin [see Fig. 3(f)].

Next, we consider the momentum distribution, which is an observable to gain information about cold atomic gas systems. The momentum distributions of the impurity for $g_{BB} = 0$ and $\omega_{AB} = 1$ are shown in Fig. 4 for different mass ratios and interaction strengths. These distributions can be understood from the discussions above. When the mass ratio increases, the impurity wave function is almost a Gaussian function, and therefore the momentum distribution will also assume a Gaussian form. Notice the characteristic oscillations in the wings of the distributions which could be very helpful for the experimental detection of the Bose polaron. The momentum distribution for majority particles is not plotted because there is no noticeable change in the distribution as we change g and/or m_{AB}.

As a final characteristic of the Bose polaron, we consider the overlap between the noninteracting and strongly interacting states for different values of g_{BB} and mass ratios as a function of N_B. This quantity is related to the orthogonality

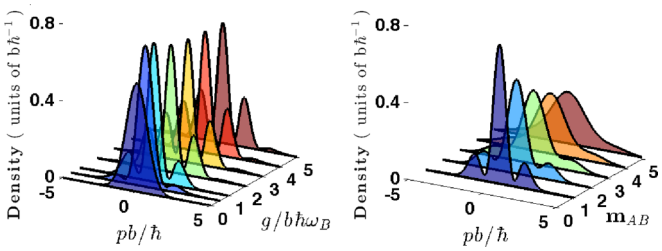

FIG. 4. (Color online) Snapshots of the momentum distribution for the impurity with different values of g for $m_{AB} = 1$ (left) and different values of m_{AB} for $g = 1$ (right). We assume $g_{BB} = 0$ and $\omega_{AB} = 1$.

catastrophe [7] and has generated recent interest as a probe of many-body physics with cold atoms [38,61,66]. In Fig. 5 we see a power-law behavior, but more interestingly, the exponent changes with both g_{BB} and mass ratio. The overlaps remain finite for finite system sizes and only go to zero for $N_B \to \infty$ [67]. The original work of Anderson [7] uses a potential to model the impurity which corresponds to the limit $m_{AB} \to \infty$. This limit shows very fast decay (high negative power dependence on N_B), similarly to what Anderson found for fermions, but already for a mass ratio $m_{AB} = 3$ the suppression is considerable, as seen in Fig. 5. On the contrary, in the opposite limit of equal masses we see much longer tails. Experiments using equal-mass two-component setups and two atomic species with different masses could therefore complement each other perfectly when studying the orthogonality catastrophe for Bose polarons.

Experiments. Our predictions should be addressable using current experimental setups. In particular, effective 1D systems have been produced that exhibit behavior consistent with zero-temperature predictions for both bosonic [14–17] and fermionic atoms [18–20]. Two-component bosonic systems in 1D [29,68,69] can be used to explore the equal-mass Bose polarons. Mass-imbalanced Bose-Bose mixtures in 1D have been explored with ^{87}Rb and ^{41}K ($m_{AB} < 1$) [26] and new experiments with ^{87}Rb and ^{133}Cs ($m_{AB} > 1$) appear promising if an effective 1D geometry can be reached [27]. Our theory provides predictions for experiments in the 1D regime,

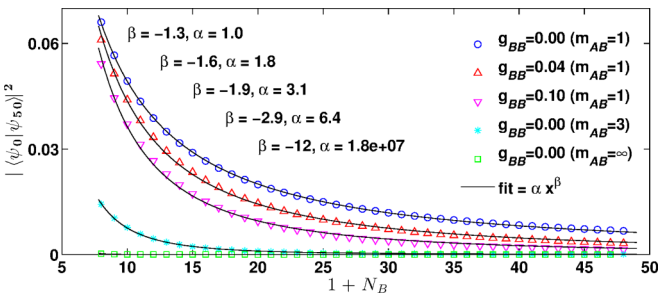

FIG. 5. (Color online) The overlap between the total wave function of the system at $g = 0$ and $g = 50$, $|\langle\psi_{g=0}|\psi_{g=50}\rangle|^2$, as a function of N_B. The best fit and the corresponding parameters are shown in the figure. The upper value of (β,α) corresponds to the upper curve, etc. For the infinite mass impurity case, the fit parameters are qualitative as there is larger uncertainty here due to the small numerical values involved.

taking into account any experimental features such as different trap frequencies for different atoms, relative displacement of the trap, and mass imbalance.

We thank M. Valiente and A. S. Jensen for feedback on the manuscript. The authors would also like to thank A. S. Jensen, D. Fedorov, C. Forssén, J. Rotureau, and E. J. Lindgren for collaboration on strongly interacting 1D systems. This work was funded by the Danish Council for Independent Research DFF Natural Sciences and the DFF Sapere Aude program. A.G.V. acknowledges partial support by Helmholtz Association under Contract No. HA216/EMMI.

[1] L. D. Landau, Phys. Z. Sowjetunion **3**, 644 (1933).
[2] L. D. Landan and S. I. Pekar, J. Exp. Theor. Phys. **18**, 419 (1948).
[3] M. D. Girardeau, Phys. Fluids **4**, 279 (1961).
[4] J. Kondo, Prog. Theor. Phys. **32**, 37 (1964).
[5] F. G. Fumi, Philos. Mag. **46**, 1007 (1955); G. D. Mahan, *Many-Particle Physics*, 2nd ed. (Plenum, New York, 1990), p. 253.
[6] W. Kohn and C. Majumdar, Phys. Rev. **138**, A1617 (1965).
[7] P. W. Anderson, Phys. Rev. Lett. **18**, 1049 (1967).
[8] H. A. Bethe, Z. Phys. **71**, 205 (1931).
[9] E. H. Lieb and W. Liniger, Phys. Rev. **130**, 1605 (1963).
[10] J. B. McGuire, J. Math. Phys. **6**, 432 (1965); **7**, 123 (1966).
[11] C. N. Yang, Phys. Rev. Lett. **19**, 1312 (1967).
[12] E. H. Lieb and F. Y. Wu, Phys. Rev. Lett. **20**, 1445 (1968).
[13] X.-W. Guan, M. T. Batchelor, and C. Lee, Rev. Mod. Phys. **85**, 1633 (2013).
[14] B. Paredes, A. Widera, V. Murg, O. Mandel, S. Fölling, I. Cirac, G. Shlyapnikov, T. W. Hänsch, and I. Bloch, Nature (London) **429**, 277 (2004).
[15] T. Kinoshita, T. Wenger, and D. S. Weiss, Science **305**, 1125 (2004).
[16] T. Kinoshita, T. Wenger, and D. S. Weiss, Nature (London) **440**, 900 (2006).
[17] E. Haller, M. Gustavsson, M. J. Mark, J. G. Danzl, R. Hart, G. Pupillo, and H. Nägerl, Science **325**, 1224 (2009).
[18] F. Serwane, G. Zürn, T. Lompe, T. B. Ottenstein, A. N. Wenz, and S. Jochim, Science **332**, 336 (2011).
[19] G. Zürn, F. Serwane, T. Lompe, A. N. Wenz, M. G. Ries, J. E. Bohn, and S. Jochim, Phys. Rev. Lett. **108**, 075303 (2012).
[20] A. N. Wenz, G. Zürn, S. Murmann, I. Brouzos, T. Lompe, and S. Jochim, Science **342**, 457 (2013).
[21] A. Schirotzek, C.-H. Wu, A. Sommer, and M. W. Zwierlein, Phys. Rev. Lett. **102**, 230402 (2009).
[22] S. Nascimbène, N. Navon, K. J. Jiang, L. Tarruell, M. Teichmann, J. McKeever, F. Chevy, and C. Salomon, Phys. Rev. Lett. **103**, 170402 (2009).
[23] C. Kohstall, M. Zaccanti, M. Jag, A. Trenkwalder, P. Massignan, G. M. Bruun, F. Schreck, and R. Grimm, Nature (London) **485**, 615 (2012).
[24] M. Koschorreck, D. Pertot, E. Vogt, B. Fröhlich, M. Feld, and M. Köhl, Nature (London) **485**, 619 (2012).
[25] P. Massignan, M. Zaccanti, and G. M. Bruun, Rep. Prog. Phys. **77**, 034401 (2014).
[26] J. Catani, G. Lamporesi, D. Naik, M. Gring, M. Inguscio, F. Minardi, A. Kantian, and T. Giamarchi, Phys. Rev. A **85**, 023623 (2012).
[27] N. Spethmann, F. Kindermann, S. John, C. Weber, D. Meschede, and A. Widera, Phys. Rev. Lett. **109**, 235301 (2012).
[28] R. Scelle, T. Rentrop, A. Trautmann, T. Schuster, and M. K. Oberthaler, Phys. Rev. Lett. **111**, 070401 (2013).
[29] T. Fukuhara, A. Kantian, M. Endres, M. Cheneau, P. Schausz, S. Hild, D. Bellem, U. Schollwöck, T. Giamarchi, C. Gross, I. Bloch, and S. Kuhr, Nat. Phys. **9**, 235 (2013).
[30] G. E. Astrakharchik and L. P. Pitaevskii, Phys. Rev. A **70**, 013608 (2004).
[31] R. M. Kalas and D. Blume, Phys. Rev. A **73**, 043608 (2006).
[32] F. M. Cucchietti and E. Timmermans, Phys. Rev. Lett. **96**, 210401 (2006).
[33] K. Sacha and E. Timmermans, Phys. Rev. A **73**, 063604 (2006).
[34] M. Bruderer, W. Bao, and D. Jaksch, Europhys. Lett. **82**, 30004 (2008).
[35] T. Johnson, M. Bruderer, Y. Cai, S. Clark, W. Bao, and D. Jaksch, Europhys. Lett. **98**, 26001 (2012).
[36] D. Benjamin and E. Demler, Phys. Rev. A **89**, 033615 (2014).
[37] W. Li and S. Das Sarma, Phys. Rev. A **90**, 013618 (2014).
[38] S. Campbell, M. A. Garcia-March, T. Fogarty, and T. Busch, Phys. Rev. A **90**, 013617 (2014).
[39] M. A. Garcia-March *et al.*, New J. Phys. **16**, 103004 (2014).
[40] A. S. Dehkharghani, A. G. Volosniev, E. J. Lindgren, J. Rotureau, C. Forssén, D. V. Fedorov, A. S. Jensen, and N. T. Zinner, Sci. Rep. **5**, 10675 (2015).
[41] J. Tempere, W. Casteels, M. K. Oberthaler, S. Knoop, E. Timmermans, and J. T. Devreese, Phys. Rev. B **80**, 184504 (2009).
[42] S. Peotta, D. Rossini, M. Polini, F. Minardi, and R. Fazio, Phys. Rev. Lett. **110**, 015302 (2013).
[43] S. P. Rath and R. Schmidt, Phys. Rev. A **88**, 053632 (2013).
[44] O. Lychkovskiy, Phys. Rev. A **89**, 033619 (2014); **91**, 040101 (2015).
[45] J. Vlietinck, W. Casteels, K. Van Houcke, J. Tempere, J. Ryckebusch, and J. T. Devreese, New J. Phys. **17**, 033023 (2015).
[46] F. Grusdt, Y. E. Shchadilova, A. N. Rubtsov, and E. Demler, arXiv:1410.2203.
[47] Y. E. Shchadilova, F. Grusdt, A. N. Rubtsov, and E. Demler, arXiv:1410.5691.
[48] A. G. Volosniev, H.-W. Hammer, and N. T. Zinner, Phys. Rev. A **92**, 023623 (2015).
[49] F. Dalfovo, S. Giorgini, L. P. Pitaevskii, and S. Stringari, Rev. Mod. Phys. **71**, 463 (1999).
[50] See Supplemental Material at http://link.aps.org/supplemental/10.1103/PhysRevA.92.031601 for a detailed derivation of our model, the definition of the density and pair-correlation function and a discussion of the effective one-dimensional Gross-Pitaevskii equation.
[51] T.-L. Ho and M. Ma, J. Low Temp. Phys. **115**, 61 (1999).
[52] D. S. Petrov, G. V. Shlyapnikov, and J. T. M. Walraven, Phys. Rev. Lett. **85**, 3745 (2000).
[53] M. Cominotti, D. Rossini, M. Rizzi, F. Hekking, and A. Minguzzi, Phys. Rev. Lett. **113**, 025301 (2014).

[54] W. Bao and Y. Cai, Kinet. Relat. Models **6**, 1 (2013).
[55] M. Olshanii, Phys. Rev. Lett. **81**, 938 (1998).
[56] H. T. Coelho and J. E. Hornos, Phys. Rev. A **43**, 6379 (1991).
[57] E. Nielsen, D. V. Fedorov, A. S. Jensen, and E. Garrido, Phys. Rep. **347**, 373 (2001).
[58] E. J. Lindgren, J. Rotureau, C. Forssén, A. G. Volosniev, and N. T. Zinner, New J. Phys. **16**, 063003 (2014).
[59] M. Barth and W. Zwerger, Ann. Phys. **326**, 2544 (2011).
[60] M. Valiente, Europhys. Lett. **98**, 10010 (2012).
[61] J. Levinsen, P. Massignan, G. M. Bruun, and M. M. Parish, Sci. Adv. **1**, e1500197 (2015).
[62] A. G. Volosniev, D. V. Fedorov, A. S. Jensen, M. Valiente, and N. T. Zinner, Nat. Commun. **5**, 5300 (2014).
[63] N. T. Zinner, A. G. Volosniev, D. V. Fedorov, A. S. Jensen, and M. Valiente, Europhys. Lett. **107**, 60003 (2014).
[64] Notice that changing the external potentials by tuning the frequency ratio ω_{AB} should yield a similar behavior.
[65] T. Busch, B.-G. Englert, K. Rzaźewski, and M. Wilkens, Found. Phys. **28**, 549 (1998).
[66] M. Knap, A. Shashi, Y. Nishida, A. Imambekov, D. A. Abanin, and E. Demler, Phys. Rev. X **2**, 041020 (2012).
[67] H. Castella, Phys. Rev. B **54**, 17422 (1996).
[68] T. Fukuhara, P. Schauß, M. Endres, S. Hild, M. Cheneau, I. Bloch, and C. Gross, Nature (London) **502**, 76 (2013).
[69] S. Hild, T. Fukuhara, P. Schauß, J. Zeiher, M. Knap, E. Demler, I. Bloch, and C. Gross, Phys. Rev. Lett. **113**, 147205 (2014).